M&C 2017 - International Conference on Mathematics & Computational Methods Applied to Nuclear Science & Engineering, Jeju, Korea, April 16-20, 2017, on USB (2017)

Multiphysics Simulation of Fuel Relocation for a Single Fuel Pin During Startup

Matthew Lund[1], Frederick N. Gleicher[2], Sebastian Schunert[3], and Mark DeHart[2]

[1]*University of Utah, Salt Lake City, UT*
[2]*Reactor Physics Design and Analysis, Idaho National Laboratory, Idaho Falls, ID*
[3]*Nuclear Engineering Methods Development, Idaho National Laboratory, Idaho Falls, ID*
matthewl.lund@utah.edu, frederick.gleicher@inl.gov, sebastian.schunert@inl.gov, mark.dehart@inl.gov

Abstract - *Analyzing light water reactor (LWR) nuclear fuel performance requires complex interlinked multi-physics, especially during nuclear reactor startup. The fuel deforms under irradiation and heating, affecting the fuel temperature, which impacts neutron interactions within the fuel. During nuclear reactor startup, initial heating of nuclear fuel causes a temperature gradient across the pellet, inducing stress in the ceramic that causes the fuel to crack in a phenomena known as fuel relocation. As the fuel relocates, the fuel-cladding gap decreases due to the increased fuel diameter, increasing heat transfer. Traditional fuel performance codes use empirical models to model neutronics, whereas MAMMOTH, a multi-physics reactor analysis tool, couples the fuel performance code BISON with the radiation transport application Rattlesnake to more precissely model the interactions. Put forth in this paper is a method for obtaining a linear heating rate from the Rattlesnake's power density distribution, which is then transfered to BISON from two different finite element fuel pin meshes to model fuel relocation during startup. Furthermore, this paper makes a comparison between a standalone BISON model using traditional empirical models and a loosely coupled BISON and Rattlesnake model using MAMMOTH for both a two-dimensional (2D) axisymmetric and full three-dimensional (3D) quarter fuel pin assembly. Both models agreed closely for the linear heat rate and pin power density with relocation occuring within the fuel rod during the first three hours of startup with similar displacements.*

I. INTRODUCTION

High fidelity modeling of light water reactor (LWR) nuclear fuel deformation, during irradiation, involves interlinked complex physics. While under irradiation, fuel rods thermally expand, cladding creeps due to irradiation, the fuel pellets swell due to fission gas, etc... [1]. These deformations affect the fuel temperature, which have an impact on the neutron interactions in the fuel. The initial heating of the pellet causes a temperature gradient between the fuel centerline and radial temperatures, inducing stress in the ceramic LWR UO_2 fuel, which eventually causes the fuel to crack, increasing the fuel diameter and volume and reducing pellet stress and fuel-cladding gap. This phenomena is referred to as fuel relocation [2], occurring within a few hours during startup, and it increases the heat transfer due to the decreased fuel-cladding gap [3]. The decrease in gap affects the local fuel temperature and the time to clad and fuel mechanical contact, which in turn has a local effect on the neutron reaction rates.

Fuel performance codes traditionally apply empirical and surrogate models for the neutron physics [4]; however, eliminating these models and coupling a fuel performance code with a neutron physics code produces simulations with higher physics fidelity [5]. Hence, Idaho National Laboratory (INL) developed MAMMOTH as a multi-physics reactor analysis tool to seamlessly couple different codes together to solve multi-physics problems [6]. For this application MAMMOTH coupled the radiation transport code Rattlesnake, which solved the diffusion equation with linear Continuos Finite Element Method (CFEM), to the fuels performance code BISON to analyze fuel relocation during startup. Presented here is a way of obtaining a linear heating rate from the power density distribution computed by Rattlesnake and transferring that linear heating rate to BISON from different finite element fuel pin meshes.

II. OVERVIEW OF MAMMOTH

MAMMOTH couples several independent applications together, including the radiation transport application Rattlesnake, the fuels performance application BISON, and the system analysis application RELAP-7, for multi-physics simulations of nuclear reactors. MAMMOTH is built upon the Multi-physics Object-Oriented Simulation Environment (MOOSE) framework, which uses finite element methods (FEM) to solve coupled nonlinear partial differential equations (PDEs) by applying the Jacobian-Free Newton Krylov (JFNK) method [7]. The framework easily scales to large problems, using massive parallelism in high-performance computing environments, and allows for one application to call multiple sub-applications (sub-apps), easily transferring data between the master application's mesh and the sub-application's mesh. MAMMOTH takes advantage of this, MOOSE's multiapp capability, allowing MAMMOTH to run multiple MOOSE-based or external sub-applications simultaneously in parallel with each MultiApp independently solving its own PDE's [8].

MOOSE provides three available types of coupling between sub-applications for multi-physics simulations: loose coupling, tight coupling using Picard iterations to resolve the coupled nonlinearities, and full implicit coupling [6]. In loose coupling, the nonlinear coupling between the master and sub-applications is not resolved. The master application solves its partial differential equations, passing the needed data to the sub-applications. The sub-applications then solve their own partial differential equations, passing the needed data back at each time step. The applications then move forward in time without resolving the nonlinear coupling. In tight coupling, each application independently solves its partial differential equations, passing the needed data to the other applications, after which Picard iterations are performed at each time-step to resolve the nonlinear coupling between each application until the solutions are below specified tolerances or the maximum number of Picard iterations. In full implicit coupling, all PDEs are solved simultaneously within a single nonlinear system of equations. MAMMOTH provides the ability to use all three coupling schemes; however, this study used loose coupling, since there was no strong two-way feedback between the neutronics and thermo-mechanics physics. This allowed each application to use its own solution strategies tailored for its own solution domain to more quickly reach convergence with a minimal number of iterations.

Rattlesnake solves the linear Boltzmann transport equation in transient, steady-state source, and critical k-eigenvalue problems. MAMMOTH adds additional tools including decay heat, burnup, linear heat flux, and power density calculations to the capabilities of Rattlesnake. BISON can be used to analyze one-dimensional spherical, two-dimensional axisymmetric, or full three-dimensional geometries for light water reactor (LWR), plate, metallic, and TRISO fuels. BISON contains models for many fuel performance phenomena that include thermal expansion, thermal and irradiation creep, fuel-cladding mechanical contact, gap heat transfer, gap/plenum pressure and volume, cracking, and relocation.

III. MODELING RELOCATION IN MAMMOTH

This study modeled relocation for a single fuel pin with dimensions from a Westinghouse 17x17 OFA assembly shown in Table I, which is designed after a modified taller Takahama-3 fuel pin [9] with an upper and lower plenum similar to newer fuel pin designs [10]. The total rod length was 464 (cm) long with a fuel diameter of .82 (cm) and gap distance of 0.016 (cm).

Component	Specification
UO_2 Fuel Pellet Height	426.72 (cm)
UO_2 Fuel Pellet Radius	.4025 (cm)
UO_2 Fuel Pellet Density	10.42 (g/cm^3)
UO_2 Enrichment	4.11 (wt%)
Fuel Volume	$2.172x10^2 \left(cm^3\right)$
Radial Gap Thickness	.0085 (cm)
Top and Bottom Cladding Thickness	2.3191 (cm)
Radial Cladding Thickness	.064 (cm)
Bottom Plenum Height	13.91 (cm)
Top Plenum Height	18.55 (cm)

TABLE I: Fuel rod specification for single pin a from a Westinghouse 17x17 assembly designed after a modified Takaham-3 fuel pin.

Two sets of meshes were used for this study: two-dimensional (2D) axisymmetric in RZ coordinates shown in Figure 1 and another full three-dimensional (3D) quarter fuel pin assembly shown in Figure 2. Each set consisted of a separate neutronics mesh for Rattlesnake and fuels mesh for BISON. The Rattlesnake fuels mesh consisted of six spectral radial rings of fuel for mapping of radial power density, a top and bottom gas plenum, a cladding of Zircaloy, a surrounding water column of 1.42063 (cm) full pitch, and a 20 (cm) water/steel top and bottom plate. The BISON mesh only included the six spectral radial fuel rings and cladding, since BISON calculates plenum and gap pressures by internal models in BISON [11]. All meshes were generated using the CUBIT mesh generation tool from Sandia National Lab [12]. The 2D axisymmetric neutronics mesh was a first order quadrilateral (QUAD4), whereas the fuels mesh was a second order quadrilateral (QUAD8) shown in Figure 1. The 3D full quarter pin neutronics and fuel meshes were both first order hexagonal (HEX8) shown in Figure 2.

The relocation model in BISON is an empirical model based on the ESCORE code [13]. This relocation model depends on fuel burnup Bu ($^{MWd}/_{MTu}$), change in pellet diameter ΔD (in), cold as-fabricated pellet diameter D_0 (in), and cold as-fabricated gap diameter G_t (in) given by:

$$\left(\frac{\Delta D}{D_0}\right) = 0.80 Q_r \left(\frac{G_t}{D_0}\right)\left(0.005 Bu^{0.3} - 0.20 D_0 + 0.3\right), \qquad (1)$$

where Q_r is a function of the linear heating rate q' given by:

$$\begin{aligned} Q_r &= 0 && \text{for} \quad q\prime \leq 6\ ^{kW}/_{ft} \\ Q_r &= (q\prime - 6)^{1/3} && \text{for} \quad 6\ ^{kW}/_{ft} \leq q\prime \leq 14\ ^{kW}/_{ft} \\ Q_r &= (q\prime - 10)/2 && \text{for} \quad q\prime \geq 14\ ^{kW}/_{ft} \end{aligned} \qquad (2)$$

The simulations ran at an operating total power of 65.81 kW for the single fuel pin for 24 hours, linearly ramping up in power from zero power with an initial cladding temperature of 600 (°C) to full power over 12 hours. Two different MAMMOTH applications were ran and compared: a standalone BISON simulation and a loosely coupled Rattlesnake and BISON simulation. Both sets of simulations used similar material models in BISON, including: fuel and cladding density, thermal fuel and cladding heat conduction, elastic fuel and cladding creep, fission gas release SIFGRS, and the relocation model. The relocation activation threshold was set at 5000 ($^{W}/_{m}$), as given by the optimization study of the relocation model by Swiler [14]. BISON's gap heat transfer LWR model was used for cladding-fuel heat transfer with a Dirichlet temperature boundary condition on the cladding of 600 (°C). All the simulations used BISON's frictionless fuel-cladding contact model.

In BISON, both fuel meshes had Dirichlet boundary condition imposed to prevent the fuel and cladding from moving in the negative axial direction and to prevent the center line of the fuel shifting within the pin, thus the pin only displaced upwards axially and outwards radially. An initial plenum pressure boundary condition applied pressure to the cladding inner walls and pellet outer surface, which increased during the simulations from the plenum pressure model. Since the 3D fuels mesh was only a quarter pin, additional boundary conditions were imposed to prevent the sides of the quarter fuel pin from moving into the direction of the missing 3/4 fuel

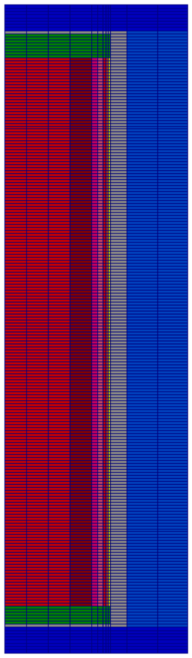

(a) Rattlesnake neutronics's mesh showing the six fuel rings in red through orange, gap in yellow, cladding in grey, water column in blue, plenum in green, and steel and water top and bottom plates in dark blue.

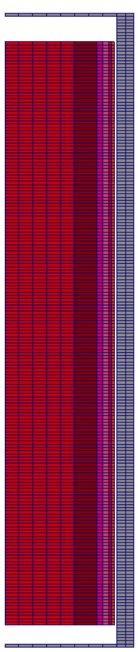

(b) Bison fuels mesh showing the six fuel rings in red through orange, gap and plenum as voids in white, and cladding in grey.

Fig. 1: 2D axisymmetric fuel pin meshes in RZ coordinate for Rattlesnake and BISON shown with the vertical axial coordinates scaled by .005.

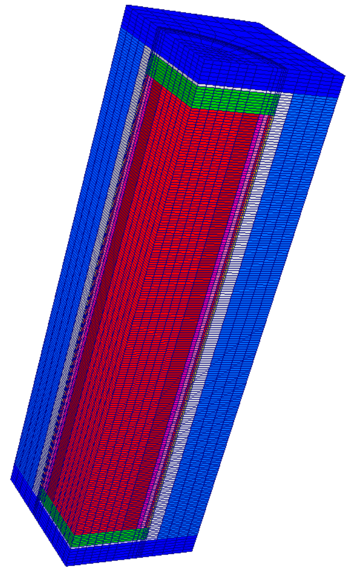

(a) Rattlesnake neutronics's mesh showing the six fuel rings in red through orange, gap in yellow, cladding in grey, water column in blue, plenum in green, and steel and water top and bottom plates in dark blue.

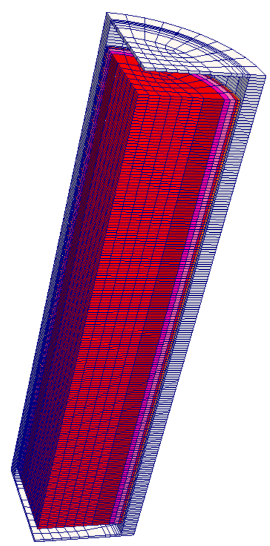

(b) BISON fuels mesh showing the six fuel rings in red through orange, gap and plenum as voids in white, and cladding in grey.

Fig. 2: 3D quarter fuel pin meshes for Rattlesnake and BISON shown with the vertical axial coordinates scaled by .005.

pin, along with Neumann boundary conditions on the temperature on both those same fuel pin sides. All simulations tracked average fission rate, burnup, power, fission gas, pellet and gap volume, and cladding temperature to verify all rates were consistent across simulations.

1. BISON Only Simulation of Relocation

In the standalone BISON application, the internal surrogate models calculated the radial power distribution, burnup, and fission rate, which were calculated based on the rod average linear power and axial power profile. The rod average linear power was calculated by:

$$q' = \frac{1}{H}\int_0^H q'(z)\,dz = \frac{q}{H}, \tag{3}$$

where q' is the linear heat rate, H is the rod height, and q is the rod total power. The calculated average linear power was $15,422\,(\mathrm{W/m})$ for the BISON only simulations; however, the value was increased to $24,640\,(\mathrm{W/m})$ so that the BISON calculated total power matched Rattlesnake's calculated power. BISON calculated the radial power profile from the rod average linear power and axial power profile using the TUBRNP model by Lassman [15, 13]. The model computed the radial power distribution based on the volumetric heat generation rate q''' for a fuel pin, which was radially and axially proportional to the fission macroscopic cross section $\Sigma_{f,k}$ for each isotope k times the flux ϕ at that point given by:

$$q'''(r) \propto \sum_k \Sigma_{f,k}\phi \tag{4}$$

The user may either provide the axial power profile in a file or as a function, such as used in this study. Since the flux axially follows a cosine distribution along the rod, the axial profile for the BISON only model was calculated by modifying Equation 4 with a cosine function as a function of the axial location z, total height of the fuel in the rod H_e, and initial total volumetric heat q_0''', which was chosen to be constant as follows:

$$q'''(r,z) = q_0''' \cos\left(\frac{\pi z}{H_e}\right) \tag{5}$$

The local linear heat rate q' is then:

$$q'(z) = \int_{A_{radial}} q'''(r,z)\,dA = \int_{A_{radial}} q_0''' \cos\left(\frac{\pi z}{H_e}\right) dA \tag{6}$$

where A is the radial area. BISON calculated the fission rate $\dot{F}$ ($^{fissions}/_{m^3 s}$) by dividing the power density P in ($^{W}/_{m^3}$) by the energy released per fission α($^{J}/_{fission}$) as shown:

$$\dot{F} = \frac{P}{\alpha} \tag{7}$$

The burnup β ($FIMA$) was calculated as a function of the volumetric fission rate $\dot{F}$, time t (s), and initial heavy metals atoms in the fuel N_f^0 ($^{heavy\,metal\,atom}/_{m^3}$) as shown [16] :

$$\beta = \frac{\dot{F}t}{N_f^0} \tag{8}$$

2. Coupling of Rattlesnake and BISON

In this study, MAMMOTH loosely coupled Rattlesnake and BISON, since there was no strong two-way feedback between the neutronics and thermo-mechanics physics. This allowed each application to use its own solution strategies tailored for its own solution domain to more quickly reach convergence with a minimal number of iterations [17, 5]. Rattlesnake calculated the power density, fission rate, linear heat rate, and local burnup mapping the results to BISON. BISON then calculated fuel thermo-mechanical properties and temperature, mapping fuel temperature back to Rattlesnake for temperature dependent cross section interpolation [6]. Rattlesnake then proceeded to the next time step, repeating the process as shown in Figure 3.

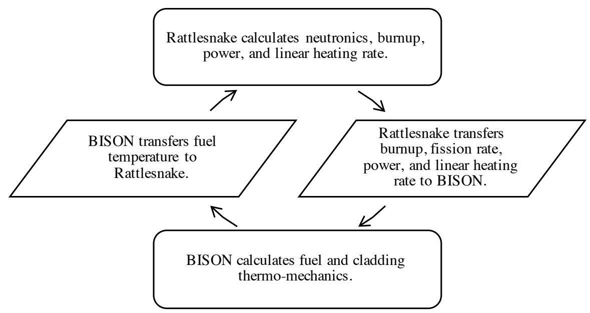

Fig. 3: Loose coupling methodology in MAMMOTH, showing calculations and transfers between Rattlesnake and BISON.

Currently Rattlesnake requires an independent lattice physics code to calculate cross sections, as MAMMOTH and Rattlesnake do not include cross section computing capabilities. Thus, DRAGON5 code created weighted multi-group neutron cross sections for the simulations [18], tabulating for the six radial fuel regions, cladding, and water cross sections as a function of burnup, fuel temperature, moderator density, and soluble boron concentration. DRAGON5 computed the axial reflector cross sections from an axial 1D homogenized calculation. The cross sections came from SHEM 361 based on ENDF/B-VII.r1 libraries [19]. The lattice calculation's fine group energy structure were condensed to two coarse energy groups to reduce run time during the simulation.

Rattlesnake solved the two group diffusion equations in depletion mode discretized with linear Continuous Finite Element Method (CFEM) in 2D and 3D, calculating groups fluxes, local burnup in each spectral region, power, and linear heat rate at each time step. MOOSE's multiapp mesh function transfer was used to map variables properly scaled between meshes, including burnup, power density, and fission rate from the neutronics mesh in Rattlesnake to the fuels mesh in BISON. For example, the fission rate is calculated based on the fission cross section and fluxes, which is then scaled by the power-scaling factor to give the true pin full power. Similarly Rattlesnake calculates the total reactor power density in $^{MW}/_{m^3}$, which must be scaled to $^{W}/_{m^3}$ for BISON.

The relocation model in Bison required the linear heating rate axially along the rod; thus an average linear heat flux method was created to determine the radial average linear heat flux $q'(z')$ in the BISON mesh, since the BISON mesh is deformable and can move. The linear heat rate is dependent on the volume integral of the volumetric heat rate of the radial elements $q'''(r,z)$ in Rattlesnake's z coordinate system, which is not movable, divided by the height of each element Δz in the Rattlesnake mesh as shown:

$$q'(z') = \int_{A_{radial}} q'''(r,z)\, dA = \frac{\int q'''(r,z)\, dV}{\Delta z} \tag{9}$$

This gave the axial linear heating rate along the rod in BISON's z' coordinate system mapped from Rattlesnake's z coordinate system, based on the initial state where the two coordinate systems overlay. The relocation model then used the linear heat rate along with the mapped burnup from Rattlesnake.

At each depletion time step from Rattlesnake, BISON then calculated the thermo-mechanical properties of the fuel. BISON used the power density from RATTLESNAKE to calculate the heat generated during fission using the neutron heat source method, which in turn changes the temperature affecting the displacement and material models. The relocation model used the linear heat rate along with the burnup from Rattlesnake. BISON's fission gas release model used the fission rate and burnup to calculate fission gas generation. After BISON calculates the fuel temperature and mechanical properties at each time step, BISON transferred the fuel temperature to Rattlesnake for the next depletion step's neutronics calculation, changing the tabulated cross sections used for the calculation.

IV. RESULTS AND ANALYSIS

1. Axisymmetric RZ Fuel Mesh

The axisymmetric RZ simulations over the first 8 hours for the coupled Rattlesnake and BISON model agree closely to the standalone BISON model. Initially both models calculated linear heat rates matched, but over time the BISON model with a cosine power distribution overestimated the linear heating rate at the center of the fuel pin shown in Figure 4, causing an increased radial displacement at the center of the fuel pin for the standalone BISON model shown in Figure 5; however, the axial position at which relocation occurs matches closely between the models as shown by the radial displacement in Figure 5. Relocation occurred in the BISON only model at around 2.5 hours, whereas in the coupled model it occurred at around 3 hours. Slight differences like these are expected due to the asymmetry in the top and bottom plenums of the Rattlesnake model. Within 8 hours, almost all the fuel within the pin experienced relocation, cracking from the temperature gradient.

The relocation of the fuel occurred for both models at the set relocation threshold of 5000 ($^W/_m$) shown in Figure 6, which shows the relocation threshold with the linear heating rate and radial displacement. At the axial points where the linear heating rate passes the relocation threshold, the radial displacement jumped due to the relocation model. As the fuel cracked due to relocation, the temperature dropped slightly axially at the locations of relocation shown in Figure 7, since the temperature showed a dip at the relocation points. This

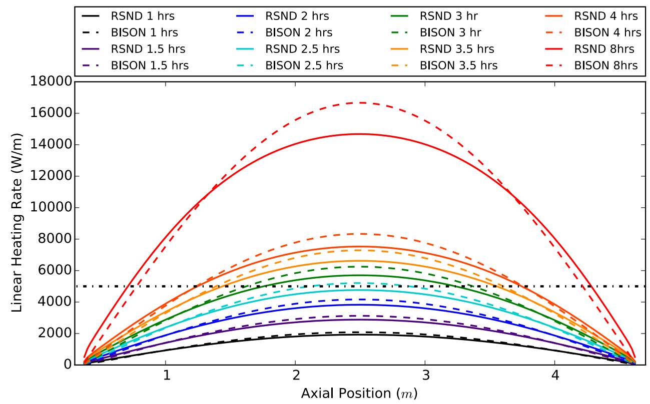

Fig. 4: Linear heating rate versus axial position for the RZ coupled Rattlesnake and RZ BISON simulation (RSND) compared to the BISON only simulations (BISON) of a fuel pin for the first 8 hours.

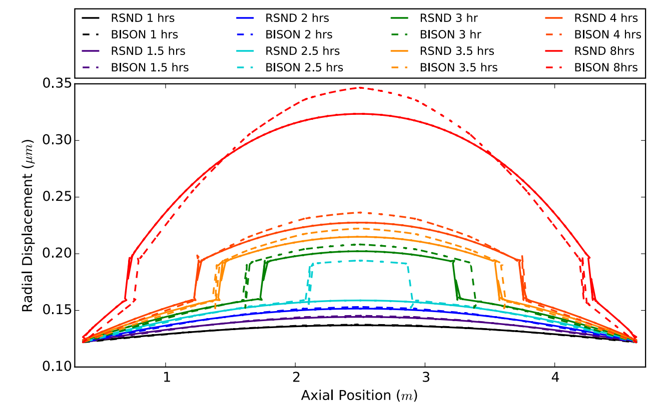

Fig. 5: Radial displacement versus axial position for the RZ coupled Rattlesnake and BISON simulation (RSND) compared to the RZ BISON only simulations (BISON) of a fuel pin for the first 8 hours.

clearly showed the increase in heat transfer between the fuel and cladding from the decreased radial gap between the two; however, the temperature change was minimal and does not affect the Doppler broadening in the neutronics calculation at the next time step.

2. 3D Quarter Fuel Pin

In the 3D quarter fuel pin simulation of a fuel pin, the linear heating rate and relocation showed similar behavior to the axisymmetric RZ model. The linear heating rate, however, shows slight variations radially across the fuel pin from the Rattlesnake neutronics calculation and extrapolation shown in Figure 8. The radial displacement for the 3D quarter pin was computed as the vector sum of the x and z component of the displacement, which was then plotted against axial position as shown in Figure 9. Both simulations in Figure 9 showed the same agreement as the axisymmetric RZ simulations in Figure 5 with relocation occurring at the same points both axially and at the same time; however, the 3D quarter pin

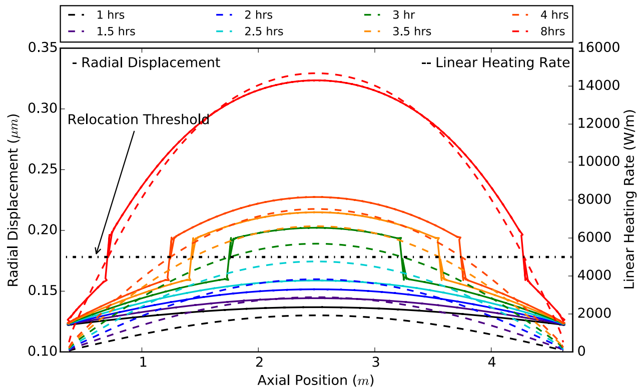

Fig. 6: Radial displacement and linear heating rate versus the axial position for the RZ coupled Rattlesnake and BISON simulation of a fuel pin for the first 8 hours.

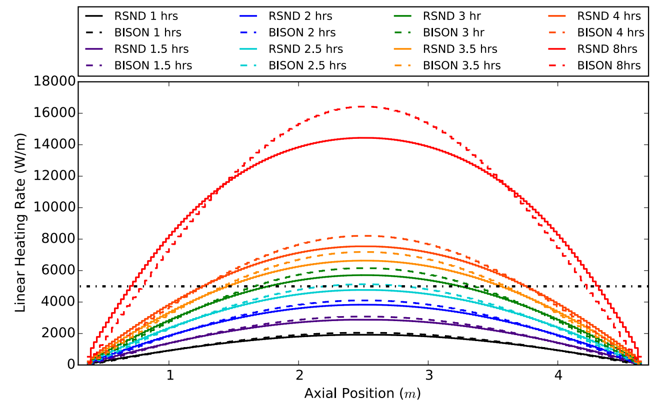

Fig. 8: Linear heating rate versus axial position for the 3D quarter fuel pin coupled Rattlesnake and BISON (RSND) compared to the BISON (BISON) simulation.

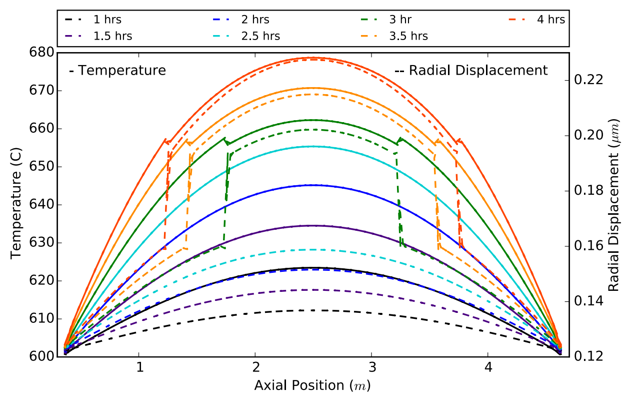

Fig. 7: Temperature and radial displacement versus the axial position for the RZ coupled Rattlesnake and BISON simulation of a fuel pin for the first 8 hours.

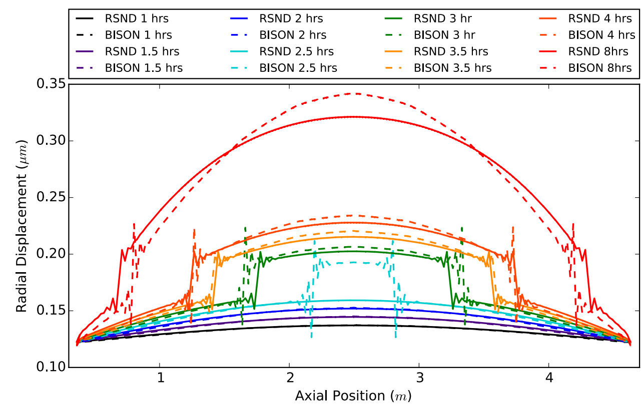

Fig. 9: Radial displacement versus axial position for the 3D quarter fuel pin coupled Rattlesnake and BISON (RSND) simulation compared to the BISON (BISON) only simulation.

simulations showed Gibb's style phenomena at the relocation and non-relocated interface. This phenomenon is expected to decrease with increased mesh density and element order.

Figure 10 shows a 3D view of the fuel pin mesh with linear heating rate with the axial axis scaled by .005 and displacements scaled by 1000. For the first 2.3 hours shown in Figure 10a, the linear heating rate is below the relocation threshold, thus the displacement of the fuel is solely due to thermal expansion. At 2.5 hours, the linear heating rate exceeds the relocation threshold and the fuel experiences a radial displacement from the relocation model shown in Figure 10b. In Figure 10c and 10d, the linear heating rate increase towards the axial ends, and the relocation model continues to expand the fuel pin due to the cracking. Figure 11 shows relocation occurred again at the anticipated relocation threshold for the 3D quarter fuel pin, shown by the jump in radial displacement where the linear heating rate reaches the line for the relocation threshold.

V. CONCLUSIONS

This study demonstrated the multi-physics capability of MAMMOTH to model the initial startup and fuel performance of a fuel pin with BISON's relocation model and Rattlesnake's neutronics calculation. Rattlesnake solved the diffusion equation with linear Continuous Finite Element Method (CFEM) in 2D and 3D and calculated the linear heat rate and pin power density with close agreement to a standalone BISON model, except for not overestimating pin power in the middle of the pin. Thus the coupled model in MAMMOTH more accurately models relocation, fuel displacement, and neutronics, because it includes temperature feedback along the fuel rod as the power shape changes over time with temperature and burnup. A standalone fuel performance code cannot capture these interlinked interactions.

The RZ fuel pin and 3D quarter fuel pin show close agreement for standalone BISON and coupled Rattlesnake and BISON simulations. For these simulations relocation occurs at the same time interval with similar displacements, thus both models in 2D and 3D model fuel relocation during startup. Relocation begins to occur within the fuel rod during the first

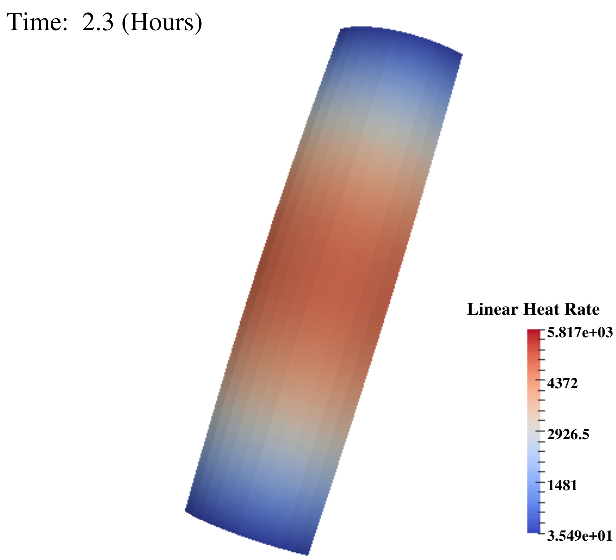

(a) 3D fuel pin at 2.3 hours during startup.

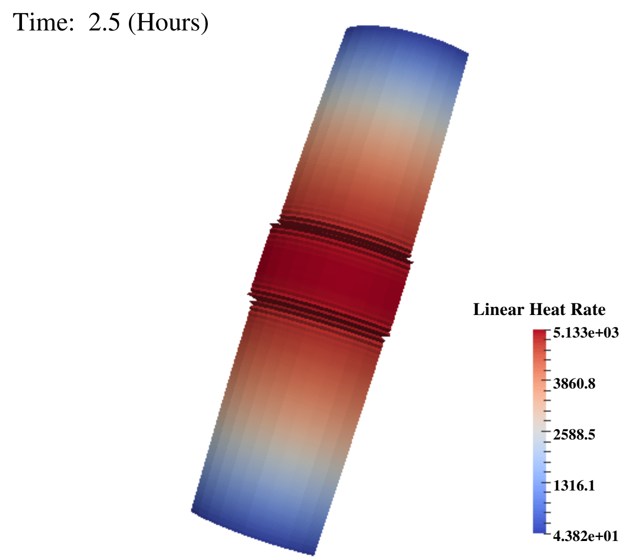

(b) 3D fuel pin at 2.5 hours during startup when relocation starts.

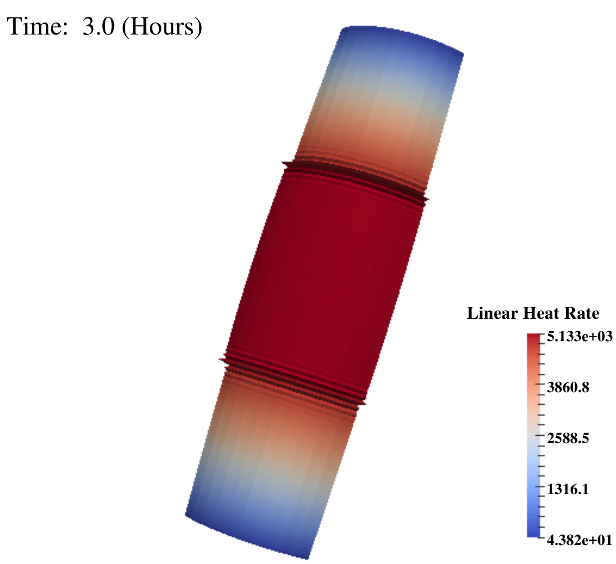

(c) 3D fuel pin at 3 hours during startup as the relocation expands axially.

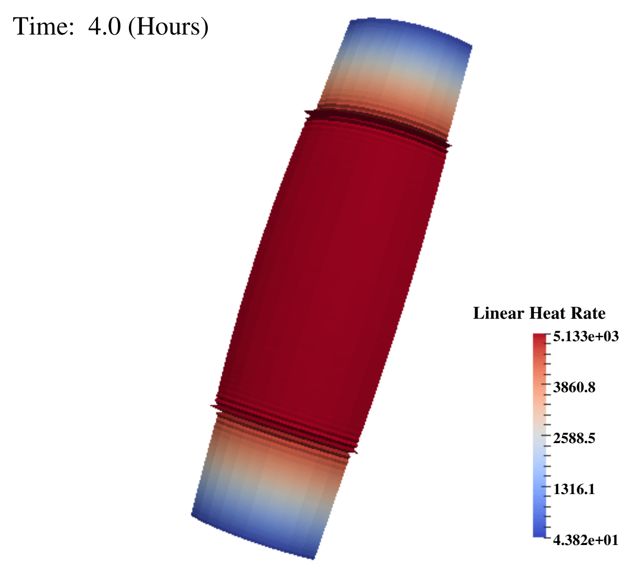

(d) 3D fuel pin at 4 hours during startup.

Fig. 10: 3D view of a fuel pin scaled by .005 in the axial direction, showing relocation versus linear heat rate for the 3D coupled Rattlesnake and BISON quarter fuel pin simulation.

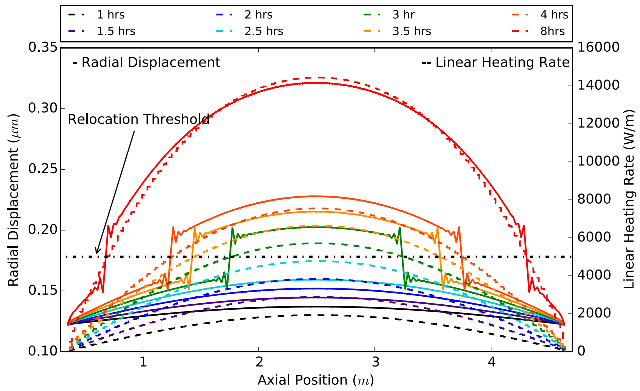

Fig. 11: Radial displacement and linear heating rate versus the axial position for the 3D coupled Rattlesnake and BISON simulation of a fuel pin for the first 8 hours. The relocation threshold is shown in a dotted dashed line at 5000 (W/m).

three hours of startup as the power is increased to full power. Most of the fuel undergoes relocation before eight hours have passed as the linear heating rate axially exceeds the set relocation threshold. A cosine axial power distribution in BISON closely resembles the neutronics calculated axial profile in Rattlesnake; however, the peak near the fuel center from the cosine axial distribution exceeds the flatter distribution from Rattlesnake, resulting in relocation occurring earlier. With onset of relocation, the change in fuel-cladding gap changes the temperature profile, which in turn affects the temperature dependent cross sections, changing the power profile and further altering the temperature profile. This essentially creates a feedback from relocation on the power profile, which is here modeled in higher fidelity than a standalone fuel performance code.

ACKNOWLEDGMENTS

We would like to thanks to the MOOSE, Mammoth, and BISON team members for their support and dedication. The submitted manuscript has been authored by a contractor of the U.S. Government under Contract DE-AC07-05ID14517. Accordingly, the U.S. Government retains a non-exclusive, royalty-free license to publish or reproduce the published form of this contribution, or allow others to do so, for U.S. Government purposes.

REFERENCES

1. B. MICHEL, J. SERCOMBE, G. THOUVENIN, and R. CHATELET, "3D fuel cracking modelling in pellet cladding mechanical interaction," *Engineering Fracture Mechanics*, **75**, *11*, 3581 – 3598 (2008), local Approach to Fracture (1986–2006): Selected papers from the 9th European Mechanics of Materials Conference.
2. M. OGUMA, "Cracking and relocation behavior of nuclear fuel pellets during rise to power," *Nuclear Engineering and Design*, **76**, *1*, 35 – 45 (1983).
3. H. STEHLE, "Performance of oxide nuclear fuel in water-cooled power reactors," *Journal of Nuclear Materials*, **153**, 3 – 15 (1988).
4. H. S. AYBAR and P. ORTEGO, "A review of nuclear fuel performance codes," *Progress in Nuclear Energy*, **46**, *2*, 127 – 141 (2005).
5. J. HALES, M. TONKS, F. GLEICHER, B. SPENCER, S. NOVASCONE, R. WILLIAMSON, G. PASTORE, and D. PEREZ, "Advanced multiphysics coupling for {LWR} fuel performance analysis," *Annals of Nuclear Energy*, **84**, 98 – 110 (2015), multi-Physics Modelling of {LWR} Static and Transient Behaviour.
6. F. N. GLEICHER, R. L. WILLIAMSON, J. ORTENSI, Y. WANG, B. W. SPENCER, S. R. NOVASCONE, J. D. HALES, and R. C. MARTINEAU, *The coupling of the neutron transport application RATTLESNAKE to the nuclear fuels performance application BISON under the MOOSE framework* (Oct 2014).
7. D. A. KNOLL and D. E. KEYES, "Jacobian-free Newton–Krylov methods: a survey of approaches and applications," *Journal of Computational Physics*, **193**, *2*, 357–397 (2004).
8. D. R. GASTON, C. J. PERMANN, J. W. PETERSON, A. E. SLAUGHTER, D. ANDRŠ, Y. WANG, M. P. SHORT, D. M. PEREZ, M. R. TONKS, J. ORTENSI, L. ZOU, and R. C. MARTINEAU, "Physics-based multiscale coupling for full core nuclear reactor simulation," *Annals of Nuclear Energy*, **84**, 45 – 54 (2015), multi-Physics Modelling of {LWR} Static and Transient Behaviour.
9. C. SANDERS and I. GAULD, *Isotopic analysis of high-burnup PWR spent fuel samples from the Takahama-3 reactor*, NUREG/CR-6798, Division of Systems Analysis and Regulatory Effectiveness, Office of Nuclear Regulatory Research, US Nuclear Regulatory Commission (January 2003).
10. "Westinghouse AP1000 Design Control Document Rev. 19 - Tier 2 Chapter 4 - Reactor - Section 4.2 Fuel System Design," Tech. Rep. ML11171A444, Westinghouse Electirc Company LLC (June 2011).
11. J. HALES, S. NOVASCONE, G. PASTORE, D. PEREZ, B. SPENCER, and R. WILLIAMSON, "BISON theory manual: The equations behind nuclear fuel analysis," *Tech-nical report, Idaho National Laboratory* (2014).
12. SNL, "CUBIT: Geometry and mesh generation toolkit," `http://cubit.sandia.gov` (2015).
13. Y. RASHID, R. DUNHAM, and R. MONTGOMERY, "Fuel analysis and licensing code: FALCON MOD01," *EPRI Report*, **1011308** (2004).
14. L. P. SWILER, R. L. WILLIAMSON, and D. M. PEREZ, "Calibration of a fuel relocation model in BISON," in "Proceedings of the International Conference on Mathematics and Computational Methods Applied to Nuclear Science and Engineering," (2013), pp. 5–9.
15. K. LASSMANN, C. O'CARROLL, J. VAN DE LAAR, and C. T. WALKER, "The radial distribution of plutonium in high burnup UO_2 fuels," *J. Nucl. Materials*, **208**, 223–231 (1994).
16. D. R. OLANDER, *Fundamental aspects of nuclear reactor fuel elements*, Technical Information Center, Energy Research and Development Administration (1976).

17. F. N. GLEICHER, B. SPENCER, S. NOVASCONE, R. WILLIAMSON, R. C. MARTINEAU, M. ROSE, T. J. DOWNAR, and B. COLLINS, *Coupling the core analysis program DeCART to the fuel performance application BISON*, American Nuclear Society - ANS; La Grange Park (United States) (Jul 2013).
18. A. HÉBERT, "{DRAGON5} and DONJON5, the contribution of École Polytechnique de Montréal to the {SALOME} platform," *Annals of Nuclear Energy*, **87, Part 1**, 12 – 20 (2016), special Issue of The 3rd International Conference on Physics and Technology of Reactors and Application.
19. A. HÉBERT, "Refinement of the Santamarina-Hfaiedh energy mesh between 22.5 ev and 11.4 kev," in "International Conference on the Physics of Reactors, Interlaken, Switzerland," (2008).